Hindawi
Advances in Materials Science and Engineering
Volume 2022, Article ID 4856089, 11 pages
https://doi.org/10.1155/2022/4856089

Research Article

A Machine Learning Approach to Optimize, Model, and Predict the Machining Factors in Dry Drilling of Nimonic C263

S. Lakshmana Kumar,[1] **V. Jacintha**,[2] **A. Mahendran**,[3] **R. M. Bommi**,[4] **M. Nagaraj**,[5] **and Umamahesawari Kandasamy**[6]

[1]*Department of Mechanical Engineering, Sona College of Technology, Salem, India*
[2]*Department of Electronics and Communication Engineering, Kings Engineering College Irrungatukottai, Chennai, India*
[3]*Department of Mechanical Engineering, Sona College of Technology, Salem, India*
[4]*Institute of ECE, Saveetha School of Engineering, SIMATS, Chennai, India*
[5]*Institute of Agriculture Engineering, Saveetha School of Engineering, Saveetha Institute of Medical and Technical Sciences, Chennai, India*
[6]*Kebridehar University, Kebridehar, Ethiopia*

Correspondence should be addressed to R. M. Bommi; rmbommi@gmail.com and Umamahesawari Kandasamy; uma@kdu.edu.et

Received 6 May 2022; Accepted 30 May 2022; Published 16 June 2022

Academic Editor: V. Vijayan

In this present paper, the machine learning approach is used to optimize, model, and predict the factors during drilling Nimonic C263 under dry mode. Nimonic C263 is tough to machine aero alloys, and it is required to find a predictive model and to optimize the factors in drilling this alloy before the actual machining process. It helps to avoid the actual machining cost and material cost. Experimental trails are planned based on Taguchi analysis, and L_{27} orthogonal array was chosen. Speed, feed, and approach angle of drill were considered as controlling factors, and cutting force and surface roughness were considered as responses. The feed forward neural network (FFNN) was used to develop a predictive model. The prediction capability was validated with a predictive model developed by Taguchi analysis. Furthermore, ANOVA (analysis of variance) analysis was done to find out the most influence factor on the responses.

1. Introduction

Nimonic C263 material is an aero material. It has great mechanical properties, and it finds usage in aeronautical parts manufacturing sectors. However, it is tough to machine owing to low thermal conductivity [1]. Therefore, suitable machining factors and cutting tools to machine this alloy are to be found out to improve the product quality. Modeling and optimization of the machining factors are an important task in machining domain. Optimization of these factors with suitable optimization tool would increase the efficiency of the machining performances and improve the product quality [2]. In manufacturing sectors, machine learning reduces cost, time, and wastages and increases the quality of the parts. It also develops systems to manage human behavior. Different machine learning algorithms are available, namely, genetic algorithm, nondominated sorting genetic algorithm, particle swarm optimization, biogeography-based optimization algorithm, firefly algorithm, artificial bee colony, gray-based Taguchi analysis, and ant colony algorithm [3, 4]. Furthermore, it also important that the machined surface may get affected severely unless the insert wear rate is controlled. The cutting fluids majorly influence to reduce the temperature in the cutting zone and control the insert wear rate. The lubrication of the machine zone with the nano-MQL (minimum quantity lubrication) lubricant system produces improved machined surface and minimum insert wear rate [5]. It is also important to note that, owing to friction in the cutting zone, temperature will be increased, and this affects tool edge and other machining

Table 1: Process parameters and their levels.

Sl. no.	Process parameters	Unit	Symbol	Levels		
				1	2	3
1	Spindle speed	rpm	N	1250	1500	1750
2	Feed rate	mm/rev	f	0.10	0.155	0.198
3	Point angle	Degree	2ρ	120	140	145

Table 2: Experiment's results.

Exp. no.	Input			Outputs	
	N (rev/min)	f (mm/rev)	2ρ (degree)	F_z (N)	R_a (μm)
1	1250	0.10	120	1250	0.576
2	1250	0.10	140	1300	0.585
3	1250	0.10	145	1375	0.592
4	1250	0.155	120	1265	0.582
5	1250	0.155	140	1360	0.592
6	1250	0.155	145	1420	0.621
7	1250	0.198	120	1385	0.595
8	1250	0.198	140	1400	0.622
9	1250	0.198	145	1430	0.641
10	1500	0.10	120	950	0.656
11	1500	0.10	140	1100	0.598
12	1500	0.10	145	1150	0.635
13	1500	0.155	120	990	0.586
14	1500	0.155	140	1110	0.642
15	1500	0.155	145	1200	0.685
16	1500	0.198	120	1060	0.552
17	1500	0.198	140	1120	0.672
18	1500	0.198	145	1175	0.695
19	1750	0.10	120	900	0.585
20	1750	0.10	140	970	0.612
21	1750	0.10	145	1000	0.651
22	1750	0.155	120	925	0.535
23	1750	0.155	140	1010	0.546
24	1750	0.155	145	1050	0.564
25	1750	0.198	120	975	0.571
26	1750	0.198	140	990	0.589
27	1750	0.198	145	1030	0.635

performances [6]. Data set was prepared by conducting milling experiments on AA7075 alloy, and the recorded data were used to develop the ANN model to predict the surface roughness. The predicted value by ANN (artificial neural network) using the small data set was compared by the Taguchi method, and the result has shown that the developed ANN model has shown best results. In ANN, back propagation and BR algorithm were used to train the data [7].

The tool wear during machining is needed to monitor in the modern machining system. Baig et al. [8] considered the vibration sign during machining and proved it as best indicators for the tool wear assessment. The ANN tool was used to predict the tool life in turning EN9 and EN24 steel with help of recorded experimental data. The ANN model was found to be effective with a coefficient of 0.99 in predicting the tool wear.

Alajmi and Almeshal [9] said that the machining performance data would be used for the prediction of the responses. They have predicted the cutting force and optimized the factors to get minimum of cutting force in turning AISI 4340 alloy. The prediction was done using Gaussian process regression, support vector machines, and artificial neural networks, and they have reported that the GPR tool has produced best prediction compared to other two prediction tools.

Uhlmann et al. [10] said that the machining process and wear of the insert have a significant impact on surface in milling process. Many approaches have been found to get models to predict surface properties during machining. However, those approaches are to be verified with a good number of experimental trails. They have suggested that the manual experimental parameterization would not be feasible; hence, a highly automated approach for the relation between tool wear and machining factors was developed using the machine learning approach. Murua et al. [11] said that the process controlling factors can be optimized with

Table 3: Response table F_z.

Level	Cutting speed	Feed rate	Point angle
(a) Response table for S/N ratio: F_z			
1	−59.61	−57.81	−57.54
2	−57.76	−58.10	−58.14
3	−56.83	−58.29	−58.52
Delta	2.78	0.48	0.98
Rank	1	3	2
(b) Response table for means: F_z			
1	677.2	555.6	539.92
2	547.8	574.2	575.9
3	492.0	587.3	602.0
Delta	185.3	31.7	62.8
Rank	1	3	2

help of predictive models, and they have developed a regression model by extracting values in face turning of inconel 718. The high-pressure coolant has reduced the wear and improves the coolant purpose compared to the traditional lubrication system.

Fertig et al. [12] presented a novel approach to predict the improvement of machined work piece during milling processes. The machine tool data were recorded, and these values were used for the development of the machine learning approach, and slicing algorithm was applied to predict the quality of the machined surface. Dubey et al. [13] have used the minimum quantity lubrication approach to turn the AISI 304 steel to determine the surface finish. Linear regression (LR), random forest (RF), and support vector machine (SVM) machine learning algorithm were used for the prediction of roughness, and the predicted values were compared with experimental results. It was finally concluded that particle size effect on surface finish and machine learning techniques were found to be far to predict roughness with minimum error.

Seleznev et al. [14] have used ceramic-based composites inserts that were used to machine nickel alloys, and they have highlighted SiAlON as best one. Furthermore, they have suggested that the new tool geometry, machining methods, and tool materials would be useful to assess the machining performance. Wei et al. [15] said that the machine learning methods are the best tool to predict the performances or characteristics of thermal transport properties. Dahbi et al. [16] have presented modeling of machining performances in turning 2017A aluminum. The data obtained in machining were used to develop the neural network, and network architecture was chosen based on R^2, MSE (mean squared error), and APE (average percentage error). Nickel-based superalloys and titanium alloy are very difficult to cut by traditional machining process because of extreme toughness and work-hardening characteristics [17–19]. When turning to Nimonic C263 superalloy, a predictive model based on DEFORM 3D was made to predict machining properties such as cutting force and the temperature of the insert cutting edge [20]. The 2D wavelet transform can break up an image of a machined surface into pictures with different levels of detail for many different surface properties, and it can be used to evaluate surfaces [21].

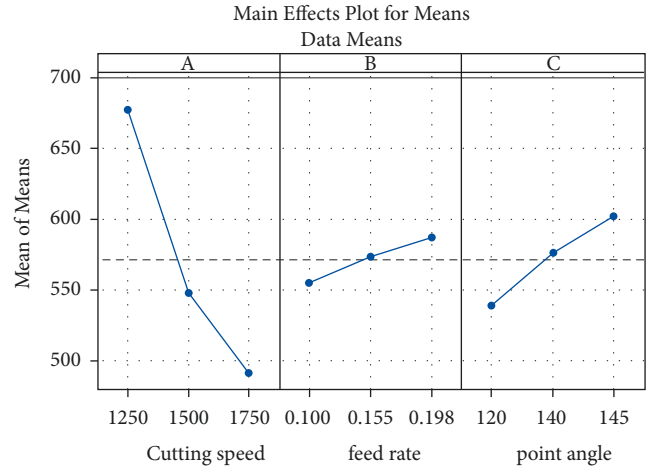

Figure 1: Main effects plot for means: cutting force.

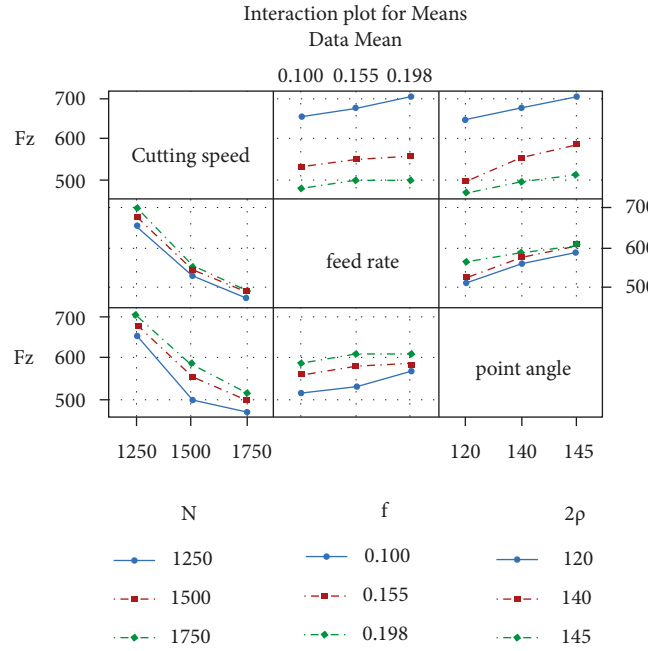

Figure 2: Interaction plot for means: cutting force.

From the literature, it is important to develop a predictive model, and there is need to optimize the process controlling factors to achieve better machining performance. Therefore, an attempt has been taken to develop a predictive model based on the machine learning algorithm using MATLAB, namely, ANN, and the model results were validated with the help of regression.

2. Materials and Methods

The work piece Nimonic C263 contains chemical composition such as 52.49 Ni, 0.19 Si, 0.46 Mn, 20 Cr, 6.29 Mo, 0.07 Cu, 1.0 Fe, 16.7 Co, 1.94 Ti, 0.48 Al, 0.04 Nb, 0.15 W, 0.02 V, 0.02 C, 0.001 S, and 0.007 Ta. The cutting force and surface roughness were considered as responses. The cutting force and surface roughness were measured using a piezo-electric

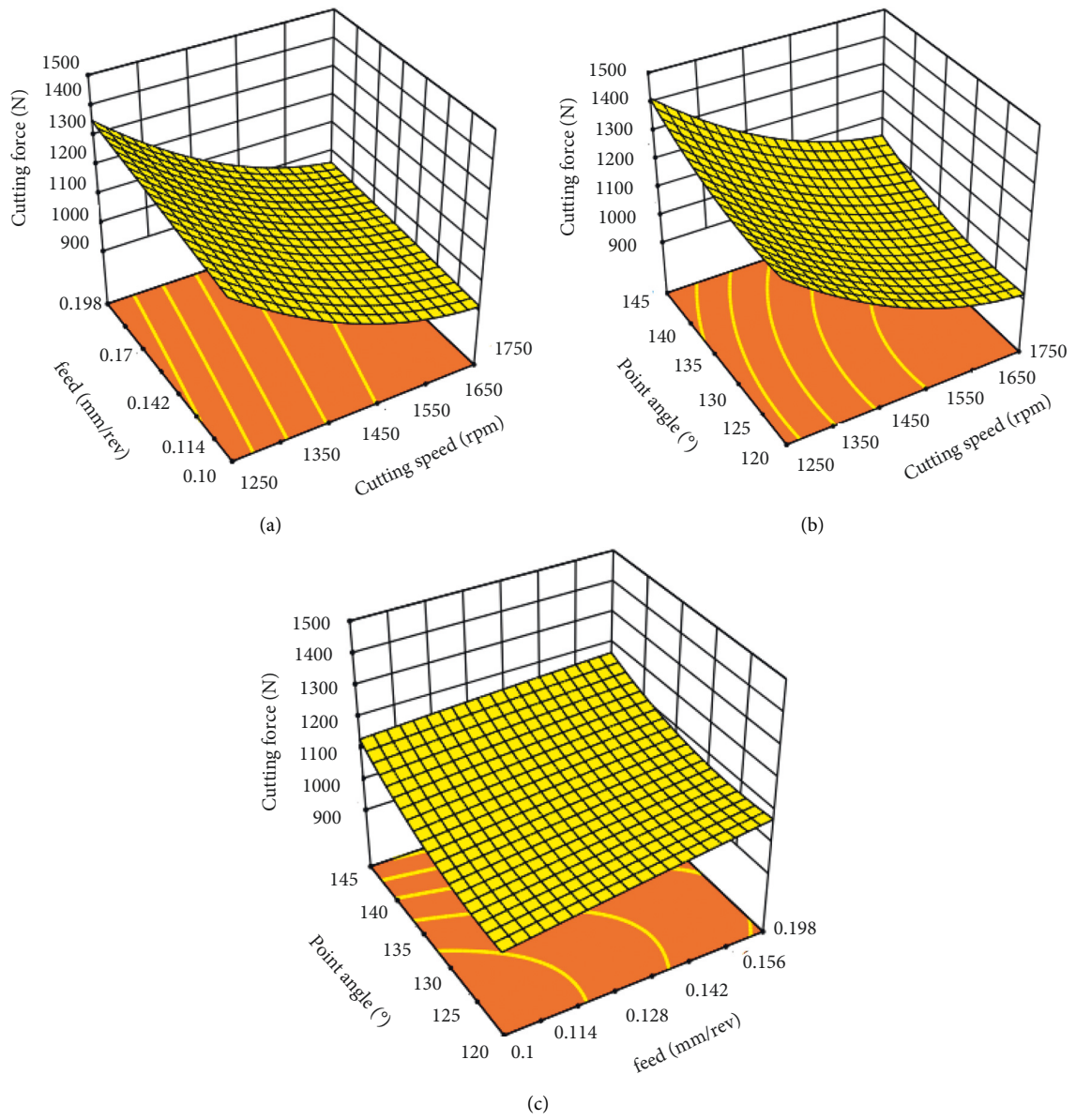

Figure 3: 3D plot for cutting force: (a) cutting speed vs. feed rate, (b) cutting speed vs. point angle, and (c) feed rate vs. point angle.

Table 4: ANOVA for cutting force.

Source	SOS	d*f*	MS	*F* value	*P* value
Model	$7.462E+05$	9	82907.42	113.34	<0.0001
N	$5.787E+05$	1	$5.787E+05$	791.17	<0.0001
F	20931.63	1	20931.63	28.62	<0.0001
2ρ	72323.10	1	72323.10	98.87	<0.0001
$N * f$	2087.67	1	2087.67	2.85	0.1094
$N * 2\rho$	76.19	1	76.19	0.1042	0.7508
$f * 2\rho$	3747.33	1	3747.33	5.12	0.0370
N^2	32511.57	1	32511.57	44.45	<0.0001
f^2	16.81	1	16.81	0.0230	0.8813
$2\rho^2$	3937.57	1	3937.57	5.38	0.0330
Residual	12435.11	17	731.48		
Cot. total	$7.586E+05$	26			
R-square: 98% and adj. R-square: 97%					

Table 5: Response table for Ra.

Level	Cutting speed	Feed rate	Point angle
Response (a) for S/N ratio: Ra			
1	4.450	4.447	4.861
2	4.102	4.556	4.360
3	4.677	4.226	4.008
Delta	0.574	0.330	0.854
Rank	2	3	1
Response (b) for means: Ra			
1	0.5994	0.5999	0.5717
2	0.6256	0.5934	0.6063
3	0.5847	0.6163	0.6317
Delta	0.0409	0.0229	0.600
Rank	2	3	1

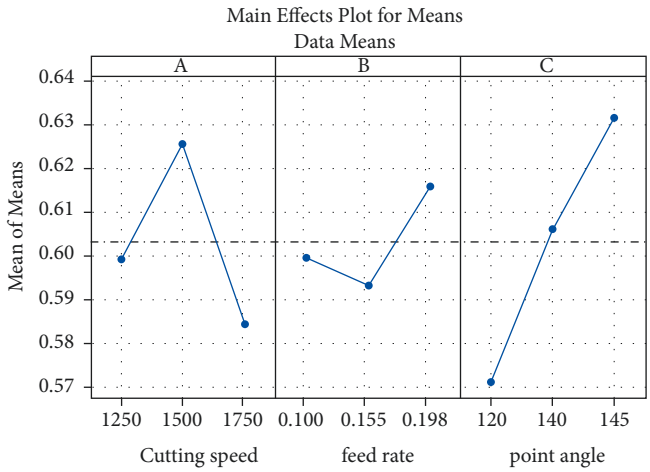

Figure 4: Main effects plot for means: cutting force.

dynamometer and Surfcom 1500 roughness tester. Taguchi analysis is implemented to design the experiments, and L27 orthogonal array was used to conduct the experiment. AlCrN-coated carbide drill is used to drill the work. The drilling factors and their levels are given in Table 1. The results of the experiment are shown in Table 2.

2.1. Development of the Predictive Model Using Regression Analysis. The regression equation was developed for the experimental values based on the following equation.

$$Y = \beta_0 + \sum_{i=1}^{k} \beta_i x_i + \sum_{i=1}^{k} \beta_{ii} x_i^2 + \sum_{i} \sum_{j} \beta_{ij} x_i x_j + \varepsilon, \quad (1)$$

where the corresponding response is "Y," x_i is the values for the i^{th} machining process parameters, and "k" is the no. of parameters to be modeled. The terms β and π are the regression coefficient and the residual of the experimental error of results, respectively. β coefficients utilised in the calculation can be determined using the least square method. ANOVA was calculated to estimate significant contribution of factors on each response. The R-squared value is used to identify the model's significance at 95% confidence interval.

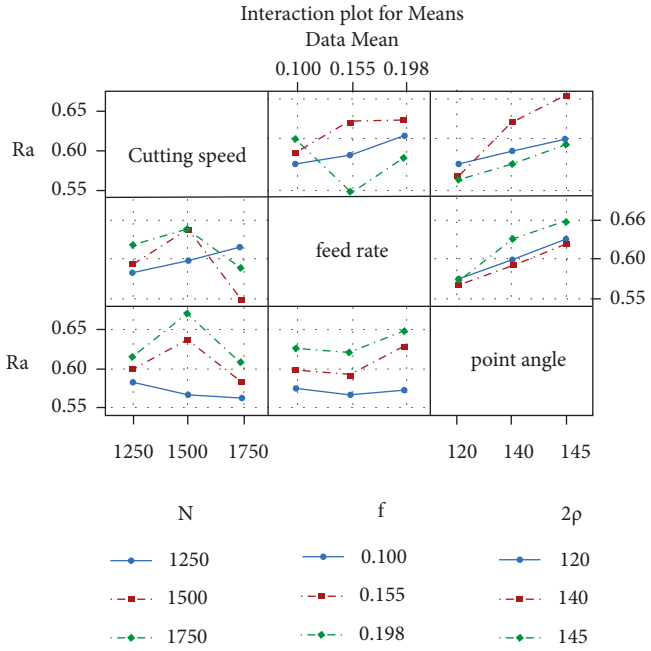

Figure 5: Interaction plot for means: cutting force.

The response table (S/N ratio and for means) for cutting force is given in Table 3, and it is observed that the cutting speed was found to be dominant on cutting force followed by point angle and feed rate.

Figures 1 and 2 show the main effects plot for force and interaction plot for means of cutting force response. Figures 3(a)–3(c) shows the three-dimensional plot for cutting force. From Figures 1–3, the cutting force magnitude is increased at lower level of cutting speed and reduced as the level of cutting speed increases. It would be owing to that the higher temperature generation at the machining zone. Further, the cutting force magnitude is increased as the level of feed rate and point angle are increased, and it could be owing to rubbing action at the cutting zone as well as at higher level of point angle and the contact surface of the drill cutting edge is more.

Furthermore, the regression analysis was done using Design–Expert software for cutting force and surface roughness. Table 4 shows ANOVA for cutting force, in which it is observed that the cutting speed has more dominant factor followed by point angle, square of cutting speed, and feed rate. Since the model developed has F value equal to 113.34 for cutting force, it is adequate to predict the cutting force. The model efficiency is confirmed by its R-squared value of 98%. As compared to point angle and feed rate, the F value is high for cutting speed (791.17), meaning that it has significant impact for force. Equation (1) is an empirical equation to predict the force.

$$\begin{aligned} F_z = {} & 1048 - 184 * N + 35 * f + 63.46 * 2\rho \\ & - 13.16 * N * f - 2.38 * N * 2\rho - 16.66 * f * 2\rho \\ & + 73.16 * N^2 - 1.70 * f^2 + 42.36 * 2\rho^2. \end{aligned} \quad (2)$$

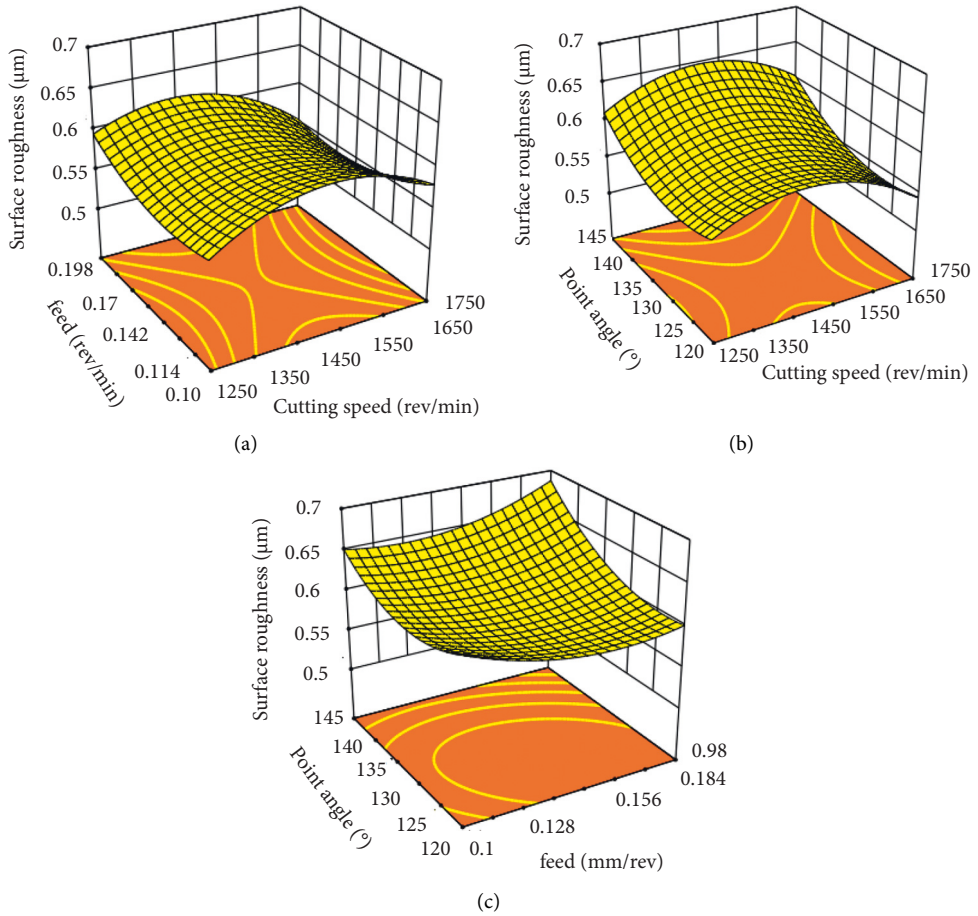

Figure 6: 3D plot for surface roughness: (a) cutting speed vs feed rate, (b) cutting speed vs point angle, and (c) feed rate vs point angle.

Table 6: ANOVA for surface roughness.

Source	SOS	df	MS	F value	P value
Model	0.0333	9	0.0037	5.00	0.0022
N	0.0008	1	0.0008	1.04	0.3215
F	0.0000	1	0.0000	0.0312	0.8619
2ρ	0.0122	1	0.0122	16.46	0.0008
$N^* f$	0.0024	1	0.0024	3.30	0.0869
$N^*2\rho$	0.0002	1	0.0002	0.2556	0.6196
$f^*2\rho$	0.0039	1	0.0039	5.26	0.0348
N^2	0.0104	1	0.0104	14.01	0.0016
f^2	0.0025	1	0.0025	3.34	0.0853
$2\rho^2$	0.0018	1	0.0018	2.43	0.1375
Residual	0.0126	17	0.0007		
Cot. total	0.0458	26			

R-square: 75% and adj. R-square: 60%

The response table (S/N ratio and for means) for cutting surface roughness in given in Table 5, and it is observed that the cutting speed was found to be dominant on the cutting force followed by point angle and feed rate. Figures 4 and 5 show the main effects plot for surface roughness and interaction plot for means of surface roughness response, respectively. Figures 6(a)–6(c) show the three-dimensional plot for surface roughness. From Figures 4–6, the surface roughness increases as the level of point angle and feed rate increases. However, the surface roughness is reduced at a high level of speed, low level of point angle, and at the middle level of feed. Furthermore, regression analysis was done using Design–Expert software for cutting force and surface roughness. Table 6 shows ANOVA for surface roughness, in which it is observed that the point angle has more dominant factor followed by cutting speed and feed rate.

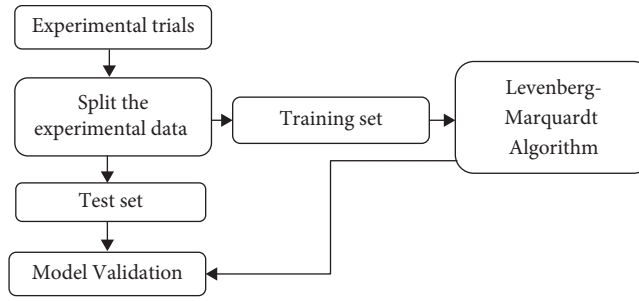

Figure 7: FFNN model flow diagram.

$$R_a = 0.5939 - 0.0067 * N + 0.0012 * f + 0.0260 * 2\rho - 0.0142 * N * f + 0.0037 * N * 2\rho + 0.0170 * f * 2\rho - 0.0416 * N^2 + 0.0206 * f^2 + 0.0286 * 2\rho^2. \quad (3)$$

Table 7: Training dataset for LM algorithm.

Exp. no.	Inputs			Target	
	N (rev/min)	f (mm/rev)	2ρ (degree)	F_z (N)	R_a (μm)
1	1250	0.10	120	1250	0.576
2	1250	0.10	140	1300	0.585
3	1250	0.10	145	1375	0.592
4	1250	0.155	120	1265	0.582
5	1250	0.155	140	1360	0.592
6	1250	0.155	145	1420	0.61
10	1500	0.10	120	950	0.565
11	1500	0.10	140	1100	0.598
12	1500	0.10	145	1150	0.635
13	1500	0.155	120	990	0.586
14	1500	0.155	140	1110	0.642
15	1500	0.155	145	1200	0.685
19	1750	0.10	120	900	0.585
20	1750	0.10	140	970	0.612
21	1750	0.10	145	1000	0.651
22	1750	0.155	120	925	0.535
23	1750	0.155	140	1010	0.545
24	1750	0.155	145	1050	0.564

Table 8: FFNN model results for test dataset using the LM algorithm.

Exp. no.	Inputs			Predicted output	
	N (rev/min)	f (mm/rev)	2ρ (degree)	F_z (N)	R_a (μm)
7	1250	0.198	120	787.1942	0.600289
8	1250	0.198	140	1086.899	0.681932
9	1250	0.198	145	1153.774	0.651407
16	1500	0.198	120	737.7439	0.597503
17	1500	0.198	140	1090.856	0.649399
18	1500	0.198	145	1106.866	0.681351
25	1750	0.198	120	738.4216	0.596766
26	1750	0.198	140	1135.186	0.555578
27	1750	0.198	145	1159.582	0.582648

Table 9: Percentage prediction errors for test dataset.

S. no.	Measured output		Predicted output		% prediction error	
	F_z (N)	R_a (μm)	F_z (N)	R_a (μm)	F_z (N)	R_a (μm)
1	1385	0.595	1387.194	0.600289	0.158178	0.881158
2	1400	0.622	1386.899	0.681932	0.944626	8.788583
3	1430	0.641	1453.774	0.651407	1.635319	1.597572
4	1060	0.552	997.7439	0.597503	6.239689	7.615499
5	1120	0.672	1090.856	0.649399	2.671686	3.480324
6	1175	0.695	1106.866	0.681351	6.155621	2.003201
7	975	0.569	938.4216	0.596766	3.897863	4.652757
8	990	0.589	987.186	0.555578	0.285049	6.015688
9	1030	0.612	1159.582	0.582648	11.1749	5.037642
Average prediction error					4.453%	3.685%

Since the model developed has F value equal to 5 for surface roughness, it is adequate to predict the surface roughness. The model efficiency is confirmed by its R-squared value of 75%. As compared to point angle and feed rate, the F value is high for cutting speed (791.17), meaning that it has significant impact for force. Equation (3) is an empirical equation to predict the force.

2.2. Implementation of the FFNN Model for the Prediction of Responses. Analysis of gradient, the individual and interacting impacts of drilling process parameters on cutting force, and surface roughness are investigated, and a quadratic regression model is built. In training a feed forward neural network, unlike Naïve computation where gradient is computed with each weight separately, in back propagation,

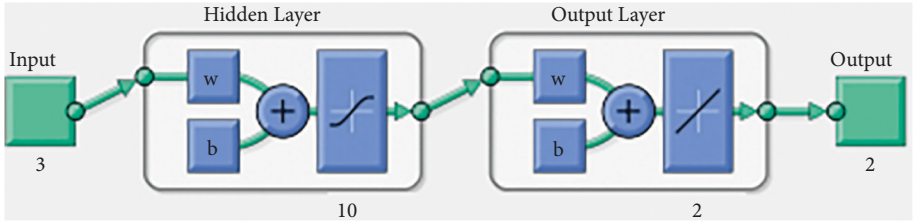

Figure 8: Feed forward neural network architecture.

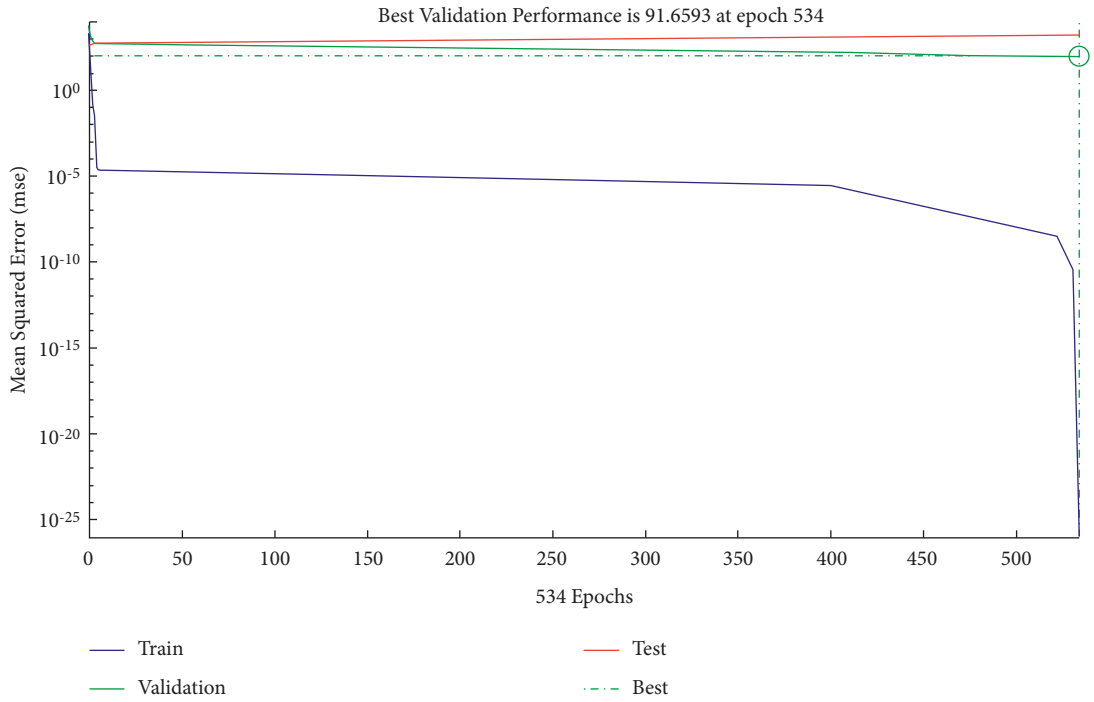

Figure 9: Performance plot of the training network.

the gradient is approximated with appropriate weights of the network for a multivariate dataset. Because of this efficiency, gradient algorithms can be used to train multilayered networks, adjusting weights to minimise loss. The back propagation algorithm works by using the chain rule to compute the gradient of the loss function with respect to each weight, one layer at a time, iterating backwards from the final layer to eliminate unnecessary calculations of intermediary terms in the chain rule, allowing it to be dynamically programmed.

The experimental trial dataset is split into two parts: testing and training. The dataset for training is utilised to adjust weights of associated neurons until the desired error level is achieved. As shown in Figure 7, training is conducted by providing a number of training vectors each with a corresponding target output vector.

Tables 7 and 8 detail the experimental conditions and findings that were utilised to train and evaluate the network. The experimental findings were utilised to train the FFNN model, with 18 experimental trials being used for training and 9 trials being used for testing. In this investigation, the feed forward back propagation algorithm with Levenberg–Marquardt approximation is utilised to train the network. In MATLAB, the neural network toolbox (nntool) was utilised to model the FFNN model. The average prediction error of the predicted output and the target output is calculated using the percentage error formula and is depicted in Table 9.

$$\text{percentage error} = \frac{|M - P|}{|P| \times 100}, \tag{4}$$

where M is the measured value and P is the predicted value.

It can be inferred from Table 9 that the average prediction error for Fz is 4.453%, and surface roughness (Ra) is 3.685%. The neuron in the input layer corresponds to the depth of cut (d), feed rate (f), and point angle. On the other hand, the surface roughness correlates to the output layer (Ra). The outputs are linked to the hidden layer neurons, while the hidden neurons are linked to the inputs. The architecture is shown in Figure 8, with three neurons in the

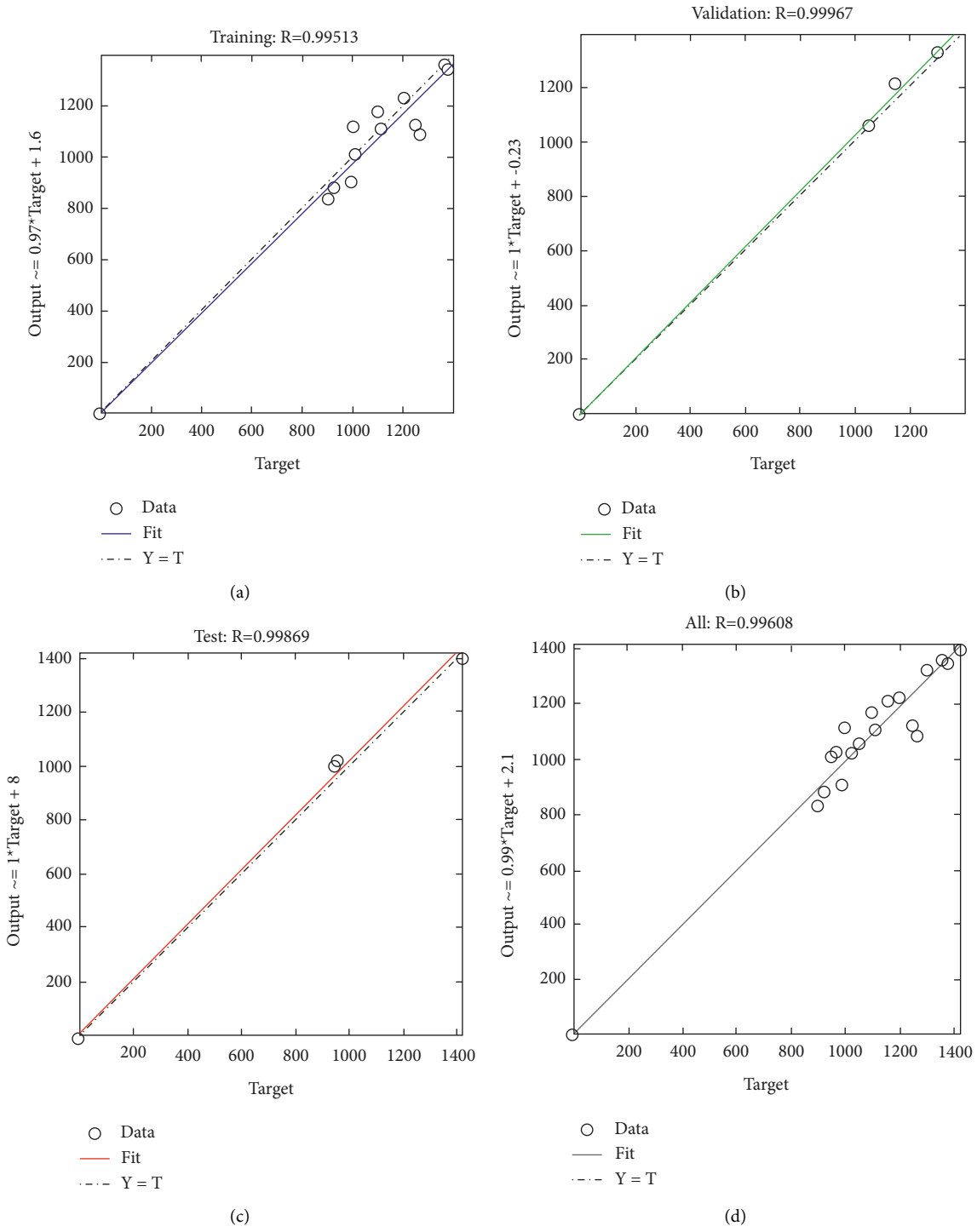

Figure 10: Regression plots of trained network w.r.t. target for (a) training, (b) validation, (c) test, and (d) all.

input layer, ten neurons in the hidden layer, and two neurons in the output layer.

Model Specification. Data division: random; training: (trainlm); Levenberg–Marquardt; performance: mean squared error (MSE) calculations: MEXEpoch: 534 iterations; gradient: $1.41e^{-11}$; Mu: $1.00e^{-09}$; validation checks: 4; and linear transfer function: purelin.

(i) One hidden layer with ten neurons

(ii) Three neurons in the input layer representing the input variables for FFNN models

(iii) Two neurons in the output layer representing the output variables independently for each of the FFNN models

Figure 9 shows the performance plot for training work initially, and for neurons in hidden layers, the purelin transfer function yielded the best results. The maximum number of training epochs was easily determined empirically using the plot network performance function plot perform. While looking at the graph of network training, it was observed that, after 534 epochs, the network training practically comes to a standstill (Figure 8).

During the training process, learning algorithms adapted the generated neural networks to the dataset. The accuracy of the fits was validated using MATLAB regression graphs (Figure 10) that showed the network outputs in relation to the objectives for testing, validation, and training sets, with values above 0.99 for all data sets. The FFNN predictive value and experiment values are compared and found to be within less than 5% error. When comparing the analytical model with the neural network model in terms of measured values obtained during experimental trials, the regression coefficient R provides a high correlation. The generated FFNNs for setting up black box models can be utilised to create a decision support system for selecting optimal parameters in drilling of superalloy Nimonic C263.

3. Conclusions

The following important conclusions were arrived in drilling of Nimonic C263 using carbide drill.

(i) The developed model by FFNN is found to be effective to predict cutting force and surface roughness compared to the regression method. As indicated by the comparatively high correlation coefficient R, the modeled neural network is well matched to the experimental data. The use of FFNN allows us to forecast surface roughness performance prediction with an accuracy of 0.9–2.9%, which is the same as the measurement values obtained during the experimental trials.

(ii) In drilling Nimonic C263, the maximum cutting force and surface roughness are observed to be 1430N and 0.65 μm respectively. The cutting speed was found to be a major factor in effecting cutting force followed by point angle and feed rate. The point angle was found to be a significant factor on surface roughness followed by cutting speed and feed rate.

Data Availability

The data used to support the findings of this study are included within the article.

Conflicts of Interest

The authors declare that they have no conflicts of interest.

References

[1] E. Chakaravarthy, S. N. Meenaskshi, A. John Presin Kumar, A. Velayudham, and B. Rishab, "Experimental analysis of process parameters in drilling nimonicC263 alloy under nano fluid mixed MQL environment," *Manufacturing Review*, vol. 8, p. 2, 2021.

[2] M. Venkatesh and R. N. Suresh Kumar, "Optimization of milling operations using artificial NeuralNetworks (ANN) and Simulated Annealing algorithm (SAA)," *Materials Today Proceedings*, vol. 5, pp. 4971–4985, 2018.

[3] A. D. Preez and G. A. Oosthuizen, "Machine Learning in cutting processes as enabler for smart sustainable manufacturing," *Procedia Manufacturing*, vol. 33, pp. 810–817, 2019.

[4] M. Manoharan, A. Kulandaivel, A. Arunagiri, M. R. A. Refaai, S. Yishak, and G. Buddharsamy, "Statistical Modelling to study the Implications of coated tools for machining AA 2014 using Grey Taguchi-based response surface methodology," *Advances in Materials Science and Engineering*, vol. 2021, Article ID 6843276, 20 pages, 2021.

[5] K. Arul and V. S. Senthil Kumar, "Effect of magneto rheological minimum quantitylubrication on machinability, wettability andtribological behavior in turning of Monel K500alloy," *Machining Science and Technology*, vol. 24, no. 5, pp. 810–836, 2020.

[6] K. Arul and V. S. Senthil Kumar, "Effects of nano cutting fluids on different machining-A Review," *International Journal of Applied Engineering Research*, vol. 10, no. 13, 2015.

[7] A. Kosarac, C. Mladjenovic, M. Zeljkovic, S. Tabakovic, and M. Knezev, "Neural-network-based approaches for optimization of machining parameters using small dataset," *Materials*, vol. 15, no. 3, p. 700, 2022.

[8] R. U. Baig, S. Javed, M. Khaisar, M. Shakoor, and P. Raja, "Development of an ANN model for prediction of tool wear in turning EN9 and EN24 steel alloy," *Advances in Mechanical Engineering*, vol. 13, no. 6, Article ID 168781402110267, 2021.

[9] M. S. Alajmi and A. M. Almeshal, "Modeling of cutting force in the turning of AISI 4340 using Gaussian process regression algorithm," *Applied Sciences*, vol. 11, no. 9, p. 4055, 2021.

[10] E. Uhlmann, T. Holznagel, P. Schehl, and Y. Bode, "Machine learning of surface layer property prediction for milling operations," *Journal of Manufacturing and Materials Processing*, vol. 5, no. 4, p. 104, 2021.

[11] M. Murua, A. Suárez, L. N. L. de Lacalle et al., "Feature extraction-based prediction of tool wear of Inconel 718 in face turning," *Insight-Non-Destructive Testing and Condition Monitoring*, vol. 60, pp. 443–450, 2018.

[12] A. Fertig, M. Weigold, and Y. Chen, "Machine Learning based quality prediction for milling processes using internal machine tool data," *Advances in Industrial and Manufacturing Engineering*, vol. 4, Article ID 100074, 2022.

[13] V. Dubey, A. K. Sharma, and D. Y. Pimenov, "Prediction of surface roughness using machine learning approach in MQL turning of AISI 304 steel by Varying Nanoparticle size in the cutting fluid," *Lubricants*, vol. 10, no. 5, p. 81, 2022.

[14] A. Seleznev, N. W. S. Pinargote, and A. Smirnov, "Ceramic cutting materials and tools suitable for machining high-temperature nickel-based alloys: a Review," *Metals*, vol. 11, no. 9, p. 1385, 2021.

[15] H. Wei, H. Bao, and X. Ruan, "Perspective: predicting and optimizing thermal transport properties with machine learning methods," *Energy and AI*, vol. 8, Article ID 100153, 2022.

[16] S. Dahbi, L. Ezzine, and H. EL Moussami, "Modeling of cutting performances in turning process using artificial neural networks," *International Journal of Engineering Business Management*, vol. 9, Article ID 184797901771898, 2017.

[17] P. Sivaprakasam and P. Hariharan, "Surface characteristics of nano powder mixed micro-wire electrical discharge machining on inconel alloy," *Materials Today Proceedings*, vol. 38, pp. 494–498, 2021.

[18] P. Sivaprakasam and P. Hariharan, "Optimization of process parameters of micro-WEDM process on inconel super alloy through response surface methodology," *International Journal of Mechanical and Production Engineering Research and Development*, vol. 8, no. 6, pp. 1001–1012, 2018.

[19] P. Sivaprakasam, P. Hariharan, and G. Elias, "Experimental investigations on magnetic field-assisted micro-electric discharge machining of inconel alloy," *International Journal of Ambient Energy*, vol. 43, no. 1, pp. 2619–2626, 2022.

[20] S. Senthil Kumar, M. P. Sudeshkumar, C. Ezilarasan, S. Palani, and J. Veerasundaram, "Modelling and Simulation of machining Attributes in dry turning of Aircraft materials Nimonic C263 using CBN," *Manufacturing Review*, vol. 8, p. 30, 2021.

[21] S. Lakshmana Kumar, M. Thenmozhi, R. M. Bommi, C. Ezilarasan, V. Sivaraman, and S. Palani, "Surface roughness evaluation in turning of Nimonic C263 super alloy using 2D DWT Histogram Equalization," *Journal of Nanomaterials*, vol. 2022, Article ID 9378487, 11 pages, 2022.